Earth and Planetary Science Letters 401 (2014) 327–336

Contents lists available at ScienceDirect

Earth and Planetary Science Letters

www.elsevier.com/locate/epsl

An oxygen isotope study of Wark–Lovering rims on type A CAIs in primitive carbonaceous chondrites

Jean-David Bodénan [a,b,*], Natalie A. Starkey [a], Sara S. Russell [b], Ian P. Wright [a], Ian A. Franchi [a]

[a] Planetary and Space Sciences, The Open University, Walton Hall, Milton Keynes, MK7 6AA, United Kingdom
[b] Department of Earth Sciences, Natural History Museum, Cromwell Road, London, SW7 5BD, United Kingdom

ARTICLE INFO

Article history:
Received 5 September 2013
Received in revised form 1 May 2014
Accepted 21 May 2014
Available online 3 July 2014
Editor: T. Elliott

Keywords:
oxygen isotopes
calcium–aluminium-rich inclusions
early Solar System

ABSTRACT

Calcium–aluminium-rich Inclusions (CAIs) and the thin Wark–Lovering (WL) rims of minerals surrounding them offer a record of the nature of changing conditions during the earliest stages of Solar System formation. Considerable heterogeneity in the gas composition in the immediate vicinity of the proto-Sun had previously been inferred from oxygen isotopic variations in the WL rim of a CAI from Allende (Simon et al., 2011). However, high precision and high spatial resolution oxygen isotope measurements presented in this study show that WL rim and pristine core minerals of individual CAIs from meteorites that had experienced only low degrees of alteration or low grade metamorphism (one from Léoville (reduced CV3), two in QUE 99177 (CR3.0) and two in ALHA 77307 (CO3.0)) are uniformly ^{16}O-rich. This indicates that the previously observed variations are the result of secondary processes, most likely on the asteroid parent body, and that there were no temporal or spatial variations in oxygen isotopic composition during CAI and WL rim formation. Such homogeneity across three groups of carbonaceous chondrites lends further support for a common origin for the CAIs in all chondrites. ^{16}O-poor oxygen reservoirs such as those associated with chondrule formation, were probably generated by UV photo-dissociation involving self-shielding mechanisms and must have occurred elsewhere in outer regions of the solar accretion disk.

1. Introduction

Understanding Solar System formation can be guided by an appreciation of the various reservoirs present in its early history, and their subsequent interactions and evolution. In light of its ubiquity (in gas, ice and dust), and involvement in many processes, oxygen cannot be ignored in models for Solar System formation. In this regard, the evidence recorded by the oxygen-bearing constituents of primitive meteorites is of critical importance. Refractory inclusions found in chondrites are invaluable tools to study O isotopes in the early Solar System as they record the conditions at the location and time of their formation. Of particular interest are calcium–aluminium-rich inclusions (CAIs); the oldest known Solar System objects (4567.2±0.6 Myr; Amelin et al., 2002; 4567.30±0.16 Myr, Connelly et al., 2012) that were formed in a short time interval (Larsen et al., 2011; MacPherson et al., 2012). They are often surrounded by thin mono- or bi-mineralic rims known as Wark–Lovering (WL; Wark and Lovering, 1977) rims. CAIs and their WL rims offer a record of conditions during the earliest stages of Solar System formation in the inner regions of the solar accretion disk (e.g. Krot et al., 2009). This is supported by their highly refractory core composition, implying high temperatures, and the presence of the short-lived radioisotope ^{10}Be, believed to originate from irradiation near the Sun, although its origin is debated (e.g. MacPherson et al., 2005 and references therein).

Refractory inclusions were formed from the earliest condensates from a hot nebula gas (MacPherson and Grossman, 1984), or molten droplets within this gas (Stolper, 1982). Most of the mineral phases present in CAIs record evidence of ^{16}O-rich solar-like O isotopic signatures (McKeegan et al., 2011), in contrast to components such as chondrules that are dominated by ^{16}O-poor signatures (e.g. Yurimoto et al., 2008 and references therein). The most generally favoured models proposed to account for O isotope heterogeneity among early Solar System objects rely on the photo-dissociation of CO molecules influenced by isotopologue-controlled self-shielding to explain the compositional variability. Different locations and times for this process to occur have been proposed such as in the molecular cloud before it collapsed (Yurimoto and Kuramoto, 2004) which would form ^{16}O-poor ices that would drift

* Corresponding author at: Planetary and Space Sciences, The Open University, Walton Hall, Milton Keynes, MK7 6AA, United Kingdom. Tel.: +44 (0) 1908 332 476.
E-mail address: jean-david.bodenan@open.ac.uk (J.-D. Bodénan).

http://dx.doi.org/10.1016/j.epsl.2014.05.035

towards the Sun after collapse. Alternatively, the inner part of the accretion disk has also been suggested as a potential location for such processes (Clayton, 2002), with the proximity to the Sun ensuring a sufficient flux of UV irradiation to drive the effect. The outer surfaces of the protoplanetary disk are also a possible location for this process to take place (Lyons and Young, 2005). Equilibration between primordial ^{16}O-poor dust and ^{16}O-rich gas has also been invoked (Krot et al., 2009) where the isotopic difference is a function of the relative average age of the gas and dust and the galactic isotopic evolution recorded in these two components. At the present time, however, it is not possible to determine the relative contributions of the proposed mechanisms.

The study of CAIs and their WL rims allows sampling of a larger timeframe and range of conditions in the early protoplanetary disk than by studying CAIs alone. The WL rims surrounding CAIs are typically 10–20 μm thick, up to a total thickness of 100 μm (Wark and Lovering, 1977), and are thought to have formed shortly after their host CAI. However, the WL rim forming processes themselves remain poorly understood. One of the proposed models (Wark and Boynton, 2001) invokes volatilisation of all but the most refractory elements of the outer CAI during a quick, high temperature "flash heating" event followed by re-introduction of elements (notably Si and Mg) lost during this event. One of the most recent models (Simon et al., 2005) suggests that WL rims formed by condensation from a gas with higher fO_2 (oxygen fugacity) and P_{Mg} (partial pressure of Mg in gas) than the environment in which the CAI cores formed. This model has been questioned by Simon et al. (2007) who found no variations in Ti valence and hence, in fO_2 between core and WL rim. Thus, it is not clear if fO_2 changed between the formation of the host CAI and its WL rim.

Considerable heterogeneity of the O isotopic composition of the gas together with turbulent movement of the CAIs in their formation region had previously been inferred from O-isotopic variations in the WL rims of a CAI from Allende (Simon et al., 2011), a meteorite known to have experienced parent asteroid aqueous alteration (e.g. Brearley, 1997). The present study focuses on samples least affected by secondary parent body or nebular processes to explore the variation in O isotope reservoirs in the inner regions of the early Solar System to understand whether isotopic variations observed in some CAIs, can be attributed to secondary processes. Understanding the level of isotopic heterogeneity in the vicinity of the CAI and WL rim formation region could have a bearing on the origin of the observed O isotope composition of early Solar System components.

2. Analytical methods

2.1. FIB-SEM

A FIB-SEM (Focused Ion Beam Scanning Electron Microscope) FEI Quanta 200 3D at The Open University (Milton Keynes, UK) was used to acquire backscattered and secondary electron images. The FIB-SEM is equipped with an Oxford Instrument X-Max X-ray detector that was used to obtain elemental energy-dispersive X-ray maps of the samples. A voltage of 20 kV was used with a probe current of 0.60 nA. Mg, Ca and Al Kα elemental maps were used to identify CAIs and their mineral phases. Quantitative analyses were also conducted on the FIB-SEM using the same beam parameters and were calibrated using a cobalt standard and an analysis time of 1 min. Only those results with a total sum of elements between 98 and 102 wt% were kept. Representative analyses of the mineral phases in the different CAIs are presented in Supplementary Tables 1 to 5.

2.2. Electron microprobe

The Cameca SX 100 electron probe micro analyser (EPMA) at The Open University was used to acquire major element compositions for melilite. An electron beam accelerated at 20 kV with an intensity of 20 nA was used for a counting time of 1 min. The beam was focused to a 2 μm spot on the sample. Only those results with a total sum of elements between 98 and 102 wt% were kept. The results are presented in Supplementary Table 6.

2.3. NanoSIMS 50L

The Cameca NanoSIMS 50L at the Open University was used to measure the O isotope ratios in the CAIs. The small spot size afforded by the NanoSIMS is useful for the samples employed in this study because the WL rims are very thin (typically 10–20 μm). A 3×3 μm raster with a pre-sputter area of 6×6 μm was selected. A probe current of 50 pA was used and sample areas were pre-sputtered for ~3 min and analyses lasted ~5 min.

A Faraday cup was used to measure ^{16}O, while ^{17}O, ^{18}O, ^{30}Si, ^{24}Mg^{16}O and ^{40}Ca^{16}O were measured on electron multipliers. Charge compensation during the analyses was achieved with an electron gun. The instrument was set to give a mass resolving power >10 000 (Cameca NanoSIMS definition, based on the measured peak width containing 80% of the ion beam; see Hoppe et al., 2013) on the ^{17}O detector, sufficient to resolve the ^{16}OH peak from that of ^{17}O (contribution of ^{16}OH typically ≤25 ppm). Typical total counts were 4×10^9 for ^{16}O, 1.6×10^6 for ^{17}O and 8×10^6 for ^{18}O. All analyses were normalised to a mineral standard matched for elemental composition to provide appropriate corrections for matrix effects and instrumental mass fractionation (IMF). O isotopes results are reported as δ^{17}O and δ^{18}O, representing permil deviations from SMOW.

Errors are reported as 2σ and combine internal precision of each analysis with the external reproducibility from standards analysed before and after typically 3 groups of 5 to 10 measurements.

The following standards were used during NanoSIMS analyses: San Carlos olivine, Burma spinel and single crystals of melilite, anorthite and diopside. The elemental composition of each standard was measured by EDX with the FEI Quanta 200 3D and their O isotope ratios were measured by laser-assisted fluorination at the Open University following the method described in Miller et al. (1999). The results are summarised in Supplementary Table 7.

For O isotope measurements, at least five spots were analysed in the standards before and after the analysis of the corresponding mineral in a sample. The typical reproducibility for the measurements demonstrated by analyses of the standard is ±2.5‰ for δ^{17}O and ±1.5‰ for δ^{18}O (2σ errors). Olivine grains from the Eagle Station pallasite were analysed to demonstrate measurement of mass independent effects and the results of these analyses are presented in Starkey and Franchi (2013) (in supplementary information).

^{24}Mg^{16}O/^{30}Si ratios measured by NanoSIMS for each point were used to obtain real-time confirmation that the analysed phase was the one expected for the selected point, and to ascertain that no drift to another phase occurred during analysis. Following NanoSIMS measurements, the position of each sputter point was checked on high resolution (~0.1 μm/px) BSE images (Supplementary Figs. 1–10). Points that sampled a mix of phases, as well as points positioned over cracks were rejected.

3. Results

3.1. Sample descriptions

Five CAIs with well-developed, or preserved, WL rims in the largely unaltered meteorites Allan Hills (ALHA) 77307, Alexandra Range (QUE) 99177 and Léoville (Figs. 1–3; Supplementary Figs. 1, 3, 5, 7, 9), were selected for this study. Each CAI was characterised using a FEI Quanta 200 3D SEM for mineralogical and chemical composition.

As this study focuses on WL rims, the dominant criteria used to select the studied CAIs were the number of mineral phases present in the rim, and the width of the rim. The CAIs presented in this study are surrounded by the largest WL rims in the studied sections of ALHA 77307, QUE 99177 and Léoville and have the highest number of phases. The WL rim areas were selected based on thickness and number of mineral phases available.

ALHA 77307 is one of the least altered members of the CO3 group, classified as a CO3.0 based on the petrology and mineralogy of amoeboid olivine inclusions (Chizmadia et al., 2002) and chondrules (Scott and Jones, 1990). In the studied section, two CAIs were analysed. The core of the first CAI, ALHA-07 (Fig. 1(a)), is composed of anhedral spinel (FeO $<$ 0.5 wt%) and minor melilite ($Åk_{12–27}$). This CAI has an elongated irregular shape, its dimensions are 350 $\times$ 240 µm and it is surrounded by a WL rim composed of a layer of diopside and a layer of olivine. The thickness of the diopside layer varies between 3 and 30 µm and contains 1.1–22.5 wt% Al_2O_3 and 0–4.3 wt% TiO_2. The WL rim olivine is forsteritic ($Fo_{93–99}$) and its thickness varies from 2 to 25 µm.

The second CAI studied in ALHA 77307, ALHA-10 (Fig. 1(b)) is an elongated irregular shaped, 315 $\times$ 175 µm sized, CAI composed of a core of anhedral spinel (FeO $<$ 0.6 wt%) and a WL rim of diopside and olivine. The layer thicknesses vary between 1 and 14 µm for olivine and 1 and 16 µm for diopside. Olivine is forsteritic ($Fo_{98–100}$) and intergrown in places with diopside. WL rim diopside contains 1.5–14.6 wt% Al_2O_3 and 0–4.3 wt% TiO_2.

The QUE 99177 meteorite (CR3.0) matrix has been described as highly pristine (Abreu and Brearley, 2010; Schrader et al., 2011), although, aqueous alteration has been reported (Bonal et al., 2013), possibly reflecting the brecciated nature of this meteorite. The meteorite is formed of a matrix made of CR3.0 material in which clasts of different meteorite lithologies are embedded (e.g. Abreu, 2013). Variations in the degree of aqueous alteration can be observed from one clast to another but significant parts of QUE 99177 escaped significant aqueous alteration and thus retained a record of its primary properties (e.g. Schrader et al., 2011). No corrosion has been observed in the metal found in this section, suggesting a very low degree of alteration, if any, for the polished thin section of QUE 99177 used in this study.

Two CAIs with WL rims were found 1 mm apart. QUE-01 has an elongated irregular shape (Fig. 2(a)), approximately 315 $\times$ 130 µm, and is composed of a spine of anhedral spinel grains typically 7 µm across and containing $\leq$0.3 wt% FeO. Surrounding the spinel is a layer of melilite ($Åk_2$ to $Åk_{14}$). A WL rim is present along the longer sides of the CAI. The WL rim sequence is composed of a thin and incomplete layer of mixed anorthite and spinel, too thin to be analysed, and a thicker diopside layer with an average thickness of around 6 µm. The diopside contains between 0.5 and 3.1 wt% Al_2O_3 and 0.2 and 1.0 wt% TiO_2.

QUE-02 has an irregular shape (Fig. 2(b)), approximately 250 $\times$ 150 µm, and is composed of a spine of anhedral spinel grains, typically 7 µm across, containing $\leq$0.3 wt% FeO. Surrounding the spinel is a layer of melilite with a composition varying between $Åk_5$ to $Åk_{16}$. A WL rim is present along the longer sides of the CAI but is absent on the shorter sides. The WL rim sequence is composed of a thin and incomplete layer of mixed anorthite and spinel, and a thicker diopside layer with an average thickness of around 6 µm. The diopside contains between 0.7 and 13.7 wt% Al_2O_3, and 0 and 3.5 wt% TiO_2. QUE-02 presents two protrusions that extend from the main CAI. The WL rim on one protrusion is very similar to the CAI interior while the diopside layer on the other is surrounded by an incomplete layer of olivine ($Fo_{98–100}$).

The discontinuity of WL rims in these two CAIs is associated with fractures showing that QUE-01 and QUE-02 were probably

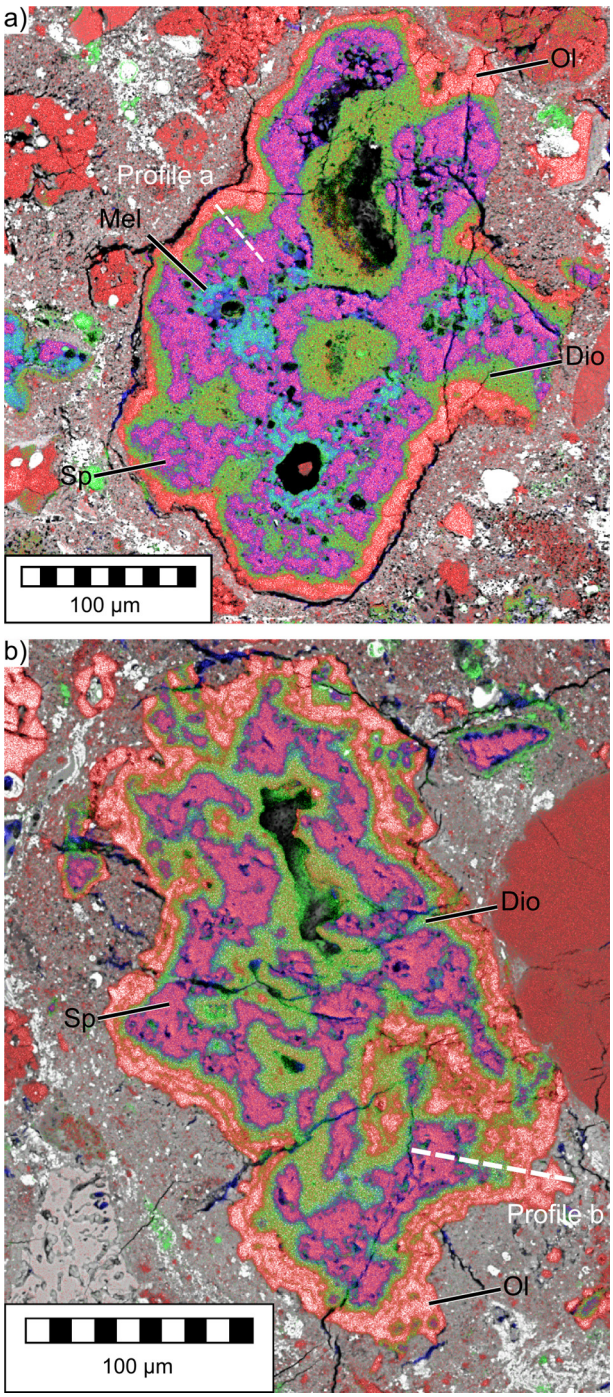

Fig. 1. Energy-dispersive X-ray maps of (a) ALHA-07 and (b) ALHA-10. Mg is coloured in red, Ca in green and Al in blue. Olivine is typically bright red; diopside is light green; spinel is purple and melilite is blue–green. The white dashed lines represent the nominal O isotope profiles. Dio = Diopside, Mel = Melilite, Ol = Olivine, Sp = Spinel. (For interpretation of the references to colour in this figure legend, the reader is referred to the web version of this article.)

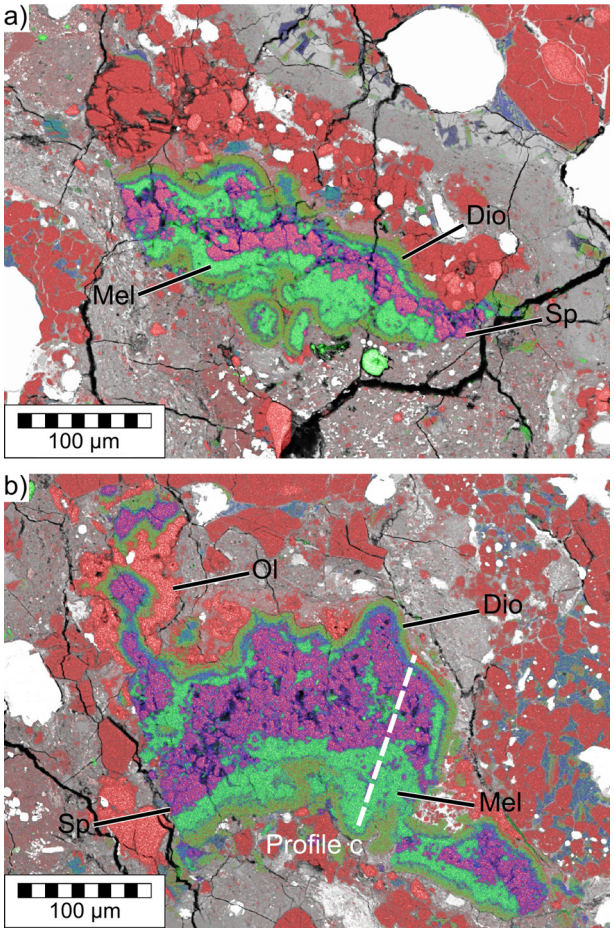

Fig. 2. Energy-dispersive X-ray maps of (a) QUE-01 and (b) QUE-02. Mg is coloured in red, Ca in green and Al in blue. Olivine is typically bright red; diopside is light green; spinel is purple and melilite is blue–green. The white dashed lines represent the nominal O isotope profiles. Dio = Diopside, Mel = Melilite, Ol = Olivine, Sp = Spinel. (For interpretation of the references to colour in this figure legend, the reader is referred to the web version of this article.)

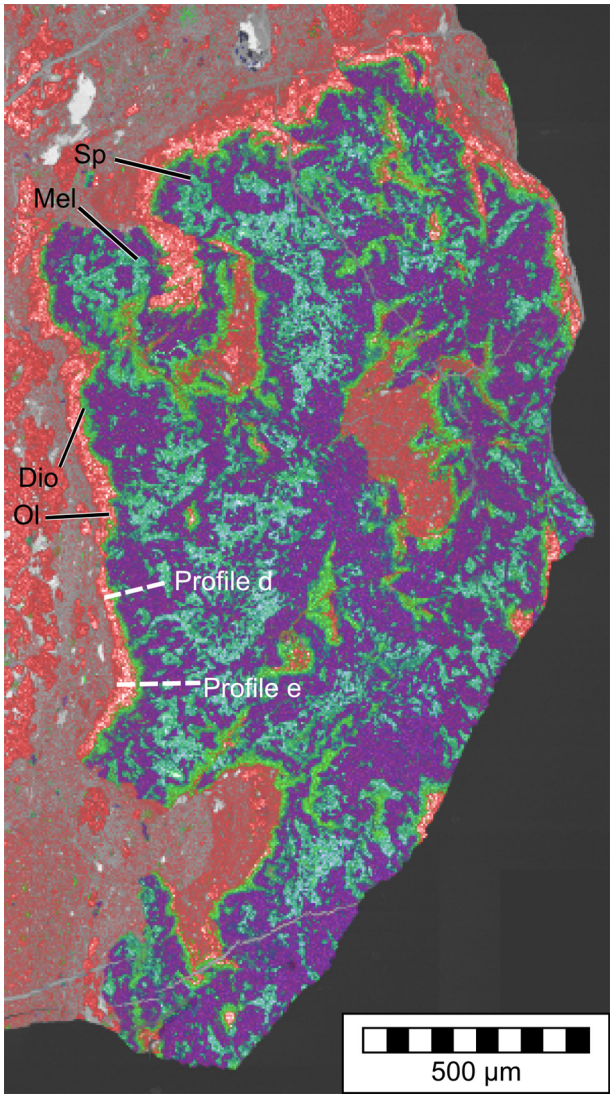

Fig. 3. Energy-dispersive X-ray map of LEO-01. Mg is coloured in red, Ca in green and Al in blue. Olivine is typically bright red; diopside is light green; spinel is purple and melilite is blue–green. The white dashed lines represent the nominal O isotope profiles. Dio = Diopside, Mel = Melilite, Ol = Olivine, Sp = Spinel. (For interpretation of the references to colour in this figure legend, the reader is referred to the web version of this article.)

once parts of one or two larger CAI(s). They also display fractures indicating that these CAIs went through an episode of brittle deformation. Some major fractures are in continuity with fractures running through the matrix suggesting that at least some of this brittle deformation took place after accretion on their parent body.

Léoville is a reduced CV3 and, as such, contains lower abundances of secondary phases than its oxidised counterparts such as Allende (Krot et al., 2004 and references therein). This may be the result of higher degrees of compaction, meaning fluids did not permeate through the rock (MacPherson and Krot, 2002), or of a heterogeneous distribution of water ice, for example. CAIs in Léoville are reported to completely lack, or contain only minor amounts of known fluid alteration phases such as hedenbergite, andradite, grossular, wollastonite, sodalite and Fe-rich olivine, as opposed to the oxidised CV3 meteorites such as Allende (Brearley, 1997; Fagan et al., 2004) in which up to 50% of melilite can be replaced by alteration assemblages (Fagan et al., 2007). The analysed thick section of Léoville is composed of chondrule material and refractory inclusions enclosed in a fine-grained matrix. The characteristic preferential orientation of the Léoville chondrite is observed in this section.

The LEO-01 CAI (Fig. 3) has an elongated shape, is 2.6×1.2 mm in size and appears to be a fragment of a larger object extending beyond the margins of the polished section. It is composed of a core of melilite ($Åk_{5-33}$), minor Ti-rich diopside and spinel surrounded by a WL rim of diopside in contact with spinel or melilite in some places, and a layer of forsteritic olivine (Fo_{97-99}) in contact with an accretionary rim or matrix. The spinel composition is very close to the pure magnesian end member (FeO $\leq$ 0.3 wt%). The diopside layer contains 4.4 to 21.4 wt% Al_2O_3, and 0.4 to 7.1 wt% TiO_2 and is 14 µm thick on average while the olivine layer is 20 µm thick on average but can reach up to 50 µm.

The absence of known secondary phases and the very low abundances of FeO (<3.6 wt%) in the different phases of ALHA-07, ALHA-10, QUE-01, QUE-02 and LEO-01 (Supplementary Tables 1–5), when it is present at all, indicates that these CAIs were not affected significantly by secondary processes.

3.2. Oxygen isotopes

The O isotope compositions of all phases in the five CAIs studied are presented in Supplementary Table 8. All CAI core and WL rim O isotope measurements for the 5 CAIs plot within error of the Carbonaceous Chondrite Anhydrous Minerals (CCAM, Clayton et al., 1977) or the Young and Russell (Y&R, Young and Russell, 1998)

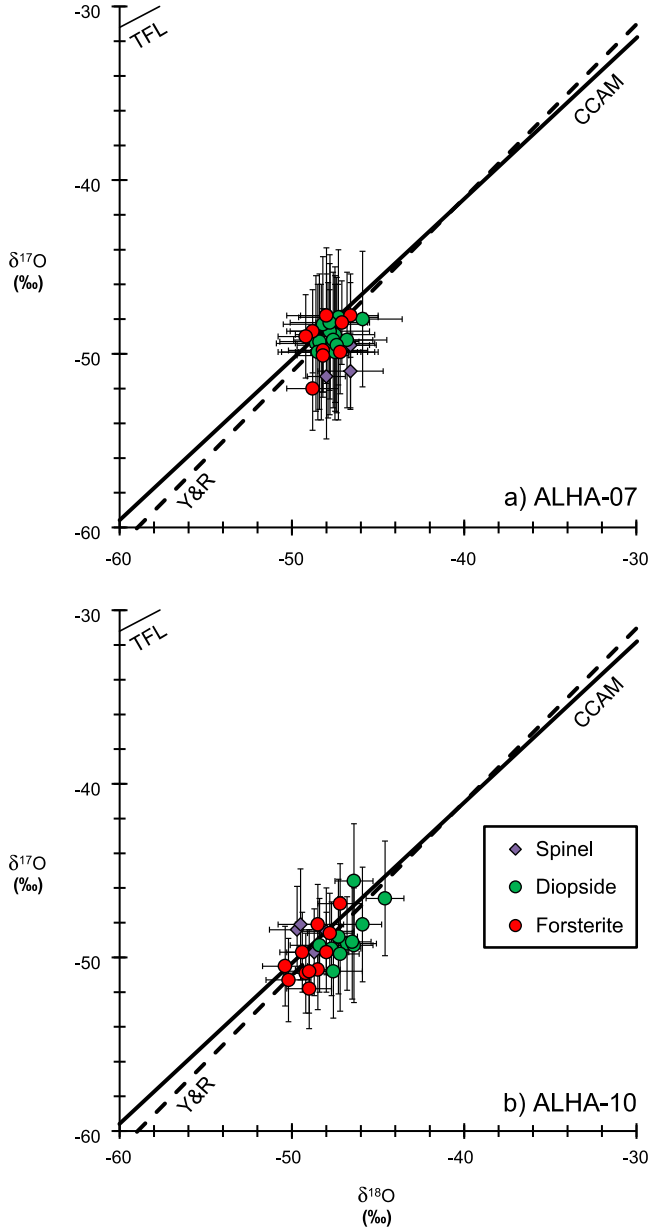

Fig. 4. Oxygen three-isotope compositions of CAI cores and rims in (a) ALHA-07 and (b) ALHA-10 plotted in an oxygen three-isotope diagram. The Terrestrial Fractionation Line (TFL, slope = 0.52), CCAM (slope = 0.94) and Y&R (slope = 1.00) lines are given for reference. Error bars are shown as 2σ. Rim minerals are symbolized by circles and core minerals by diamonds.

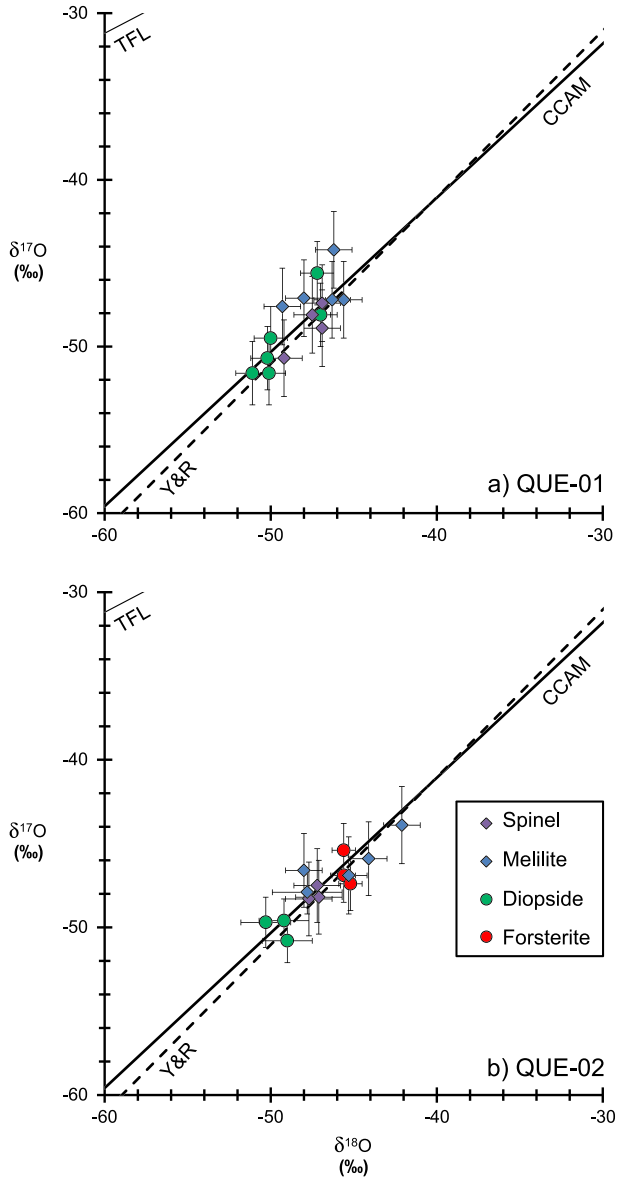

Fig. 5. Oxygen three-isotope compositions of CAI cores and rims in (a) QUE-01 and (b) QUE-02 plotted in an oxygen three-isotope diagram. The Terrestrial Fractionation Line (TFL, slope = 0.52), CCAM (slope = 0.94) and Y&R (slope = 1.00) lines are given for reference. Error bars are shown as 2σ. Rim minerals are symbolized by circles and core minerals by diamonds.

lines (Figs. 4, 5 and 6). This indicates that these CAIs have not been significantly affected by mass-dependent fractionation processes.

Minerals in ALHA-07 and ALHA-10 have an average $\Delta^{17}O = -24.5 \pm 2.1(2\sigma)‰$, and $\Delta^{17}O = -24.3 \pm 2.4(2\sigma)‰$, respectively (Table 1). Values for diopside, spinel and olivine cluster tightly on a three-isotope-diagram around $\delta^{17}O = -49‰$ and $\delta^{18}O = -48‰$ for both CAIs (Fig. 4).

The $\Delta^{17}O$ values of all the minerals in the two CAIs found in QUE 99177 (QUE-01 and QUE-02) have average $\Delta^{17}O$ values of $-23.4 \pm 3.1(2\sigma)‰$ and $-23.2 \pm 1.9(2\sigma)‰$ respectively. While WL rim minerals and core spinel in LEO-01 show similar $\Delta^{17}O$ values, with an average $\Delta^{17}O = -23.0 \pm 2.0(2\sigma)‰$, melilite extends to ^{16}O-poor compositions (up to $\Delta^{17}O = -2.7 \pm 3.0(2\sigma)‰$) falling along the CCAM line (Fig. 6). Such variation is commonly observed in CAIs from other CV meteorites.

Spinel is the phase that is most resistant to isotopic exchange and has identical isotopic composition, within error, across all five CAIs with an average $\Delta^{17}O = -23.6 \pm 2.5(2\sigma)‰$. Melilite is variable when LEO-01 is taken into account (average $\Delta^{17}O = -13.1 \pm 16.7(2\sigma)‰$) but is far more homogeneous and closer to spinel values when only considered in the CAIs from QUE 99177 (average $\Delta^{17}O = -22.4 \pm 2.1(2\sigma)‰$). WL rim diopside and olivine in the five studied CAIs have a remarkably homogeneous O composition. The average value for diopside across the samples is $\Delta^{17}O = -23.9 \pm 2.5(2\sigma)‰$, which is also the average value for olivine (see Table 1).

To evaluate O isotopic changes across the WL rims and the CAI interiors, profiles were built (Figs. 1–3 and 7) using O isotope values from spot analyses. The complex mineralogy and fractured nature of the CAIs meant that O isotope analyses could not be performed along simple transects. Instead, the location of each point was projected onto a nominal line to form the profile across the

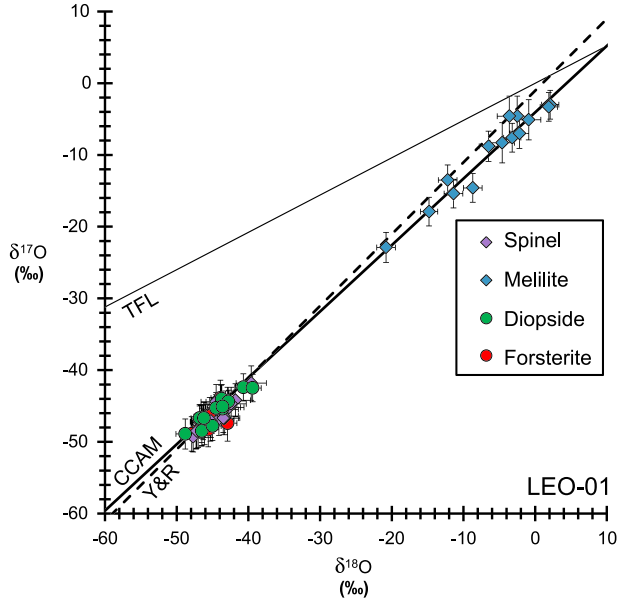

Fig. 6. Oxygen three-isotope compositions of CAI cores and rims in LEO-01 plotted in an oxygen three-isotope diagram. The Terrestrial Fractionation Line (TFL, slope = 0.52), CCAM (slope = 0.94) and Y&R (slope = 1.00) lines are given for reference. Error bars are shown as 2σ. Rim minerals are symbolized by circles and core minerals by diamonds.

CAI and its WL rim. In profiles a and b from ALHA-07 and ALHA-10 (Fig. 7), respectively, the maximum distance of spots from the nominal line is 20 µm. For profile c in QUE-02, projected points were up to 40 µm from the nominal lines. To build profiles d and e in LEO-01, points up to a distance of 60 µm, and 85 µm, respectively, were projected onto the nominal lines.

4. Discussion

4.1. Secondary alteration effects in the CAIs

All core minerals studied in the two CAIs from the ALHA 77307 (CO3.0) section are ^{16}O-rich (Fig. 4). The O isotopic compositions of spinel and melilite are very similar to those previously measured in fine-grained unaltered CAIs found in the Yamato-81020 (CO3.0) and Kainsaz (CO3.1–3.2) CO meteorites (Itoh et al., 2004). In the core of some CAIs from the more altered of the two CO3 meteorites used in that study, Kainsaz, secondary phases that are usually accompanied by ^{16}O depletion have developed.

Aléon et al. (2002) reported O isotope compositions for CAIs in CRs spanning a range of degrees of alteration, as indicated by petrographic and whole-rock oxygen isotopic compositions (e.g. Schrader et al., 2011). The O isotope compositions of most of these CAIs are similar to those measured in QUE-01 and QUE-02, but some have ^{16}O-poor values that cover a range from −50‰ to −30‰ in δ^{18}O and δ^{17}O. In contrast, the CAIs QUE-01 and QUE-02 from the CR meteorite QUE 99177 cluster more tightly between −52‰ and −44‰ (Fig. 5). QUE 99177 has the most ^{16}O-rich whole-rock signature among CRs, indicative of a lower degree of exchange of its components with the parent body (Schrader et al., 2011). The combined evidence from the CO and CR meteorites, groups where there is considerable range from heavily altered through to almost unaltered samples, indicates that narrower ranges of O composition are observed in the CAIs that have experienced the least aqueous and/or thermal alteration. This suggests that secondary processing on the asteroid parent bodies contributes to the oxygen isotopic composition of the CAIs.

In the large type A CAI studied by Simon et al. (2011) in Allende, melilite displays a clear pattern of increasing enrichments of ^{17}O and ^{18}O towards the rim over the outer ∼50 µm, indicative of exchange between an external ^{16}O-poor reservoir and a ^{16}O-rich interior. These authors argued that the observed profile could be modelled by solid–gas exchange processes between 1000 and 1600 K for durations between ∼530 000 (at 1200 K) and ∼500 yrs (at 1600 K). Numerous short heating events may have occurred in the early Solar System (Young et al., 2005) that could be responsible for the observed isotopic exchange. The much lower oxygen diffusion rate in most of the other phases present in the CAI left them largely unaffected by this event. In the case of LEO-01, the ^{16}O-poor melilite was observed up to an apparent distance of 150 µm from the WL rim, that may also be the result of short heating events under similar conditions to those observed in the Allende CAI studied by Simon et al. (2011). However, there is no apparent systematic O isotopic variation with distance from the WL rim in LEO-01, although the complex shape of LEO-01 makes it difficult to estimate the true distance to the WL rim.

Heterogeneous O isotopic compositions of melilite in some type A and B CAIs have been explained by rapid heating and cooling of CAIs in a ^{16}O-poor gas reservoir, possibly during repeated events (e.g. Yurimoto et al., 1998; Fagan et al., 2004; Harazono and Yurimoto, 2003; Ito et al., 2004). Greenwood (2004) demonstrated that the melting of melilite is kinetically favoured relative to other CAI mineral phases. Thus, moderate heating events in the nebula may preferentially melt this phase, greatly enhancing its exchange rate with the surrounding ^{16}O-depleted gas. Such events and gas reservoirs may be associated with the later chondrule formation events (e.g. Yurimoto et al., 2008). The short duration and moderate temperatures would leave other phases unmelted and, therefore, largely unaffected by exchange. This process could have affected LEO-01 as it is a Type A CAI that appears to have experienced some re-melting. Both of these processes, solid–gas or liquid–gas exchange, could explain the ^{16}O-poor compositions in melilite and could have left the more resilient phases unaffected.

Variation in O isotopic composition in melilite in CAIs has also been linked to condensation of the melilite from a gas phase with an evolving O isotope signature (Katayama et al., 2012). The melilite in LEO-01 displays an apparent correlation between O isotopic composition and åkermanite content that parallels that observed in the CAIs from Vigarano (Katayama et al., 2012) and Efremovka (Kawasaki et al., 2012), where condensation has been proposed as the controlling factor. However, in the case of LEO-01, the trend is weak and most of the points are within error of each other (Supplementary Fig. 11) with no pattern related to proximity to the margin of the CAI. It is, therefore, unclear if there is a common origin for the variable O isotopic composition of melilite in these three CAIs from reduced CV3 meteorites.

While the aforementioned processes are plausible to explain the exchange of melilite in LEO-01 with a ^{16}O-depleted isotope reservoir, they are deemed unlikely. There is evidence that this exchange must have occurred some time after WL rim formation was complete, as the identical O isotope compositions of spinel in the core and olivine in the WL rim strongly argues for a common source. Modification of melilite prior to WL rim formation would require rapid transfer of the CAI to a ^{16}O-poor reservoir and back to the original ^{16}O-rich reservoir (or rapid evolution of the surrounding gas reservoir) during the short time interval between core and WL rim formation.

4.2. Primary oxygen isotopic composition of the CAI Cores and WL Rims

The five O isotope composition profiles acquired in the studied CAIs (Figs. 1–3, 7) show no variation in Δ^{17}O across the WL rim sequences, or between the WL rim and the core minerals (with the

Table 1
Summary table of average $\Delta^{17}O$ for each phase in individual CAIs and across the samples with n = number of analyses for one phase and σ = standard deviation.

Sample	$\Delta^{17}O$ (‰)					
	Core		Rim			
Stat	Melilite	Spinel	Diopside	Olivine		All
ALHA-07						
n =	n.a.	4	18	9		31
mean =	n.a.	−25.9	−24.3	−24.3		−24.5
2σ =	n.a.	1.6	1.5	2.4		2.0
ALHA-10						
n =	n.a.	4	11	11		26
mean =	n.a.	−23.2	−24.4	−24.5		−24.3
2σ =	n.a.	1.8	2.4	2.4		2.4
QUE-01						
n =	5	4	6	n.a.		15
mean =	−22.2	−24.0	−23.9	n.a.		−23.4
2σ =	2.6	2.0	3.2	n.a.		3.1
QUE-02						
n =	5	3	3	3		14
mean =	−22.6	−23.4	−24.3	−22.9		−23.2
2σ =	1.5	0.9	1.8	2.2		1.9
LEO-01					*Without Mel*	*With Mel*
n =	14	20	16	12	48	62
mean =	−6.5	−23.1	−23.3	−22.6	−23.0	−19.3
2σ =	5.8	2.0	1.9	2.0	2.0	14.3
ALL CAIs						
n =	24	35	39	50		148
mean =	−13.1	−23.6	−23.8	−23.9		−22.0
2σ =	16.7	2.5	2.4	2.5		10.5

N.a. – not analysed.

exception of melilite in LEO-01 as discussed above). The flat $\Delta^{17}O$ profiles indicate that all phases in the WL rim and the cores of the CAIs studied here sampled the same original isotopic reservoir, with a $\Delta^{17}O = -23.5 \pm 2.5(2\sigma)$‰ (average of all spinel measurements in the 5 CAIs, see Table 1).

The flat $\Delta^{17}O$ profiles across the CAI interiors and WL rims (Fig. 7) in this study imply that the CAIs remained in the same reservoir for the entire period of CAI and WL rim formation. These results are in stark contrast to the previous results from Simon et al. (2011) that showed large variations in O isotope composition across WL rim sodalite, pyroxene and olivine in a CAI from Allende. Sodalite is a known product of Ca–Fe-alkali alteration of CAIs, implying that this CAI went through an episode of alteration on the parent body (Krot et al., 2009). As there is evidence for the water involved in secondary alteration of the Allende parent body being strongly depleted in ^{16}O (e.g. Rowe et al., 1994; Maruyama et al., 1999; Choi et al., 2000; Hua et al., 2004; Cosarinsky et al., 2008; Rudraswami et al., 2011; Jogo et al., 2013), the O isotope variations observed in the Allende CAI WL rim (Simon et al., 2011) are unlikely to reflect the primary composition of the reservoir(s) in which the CAI and its WL rim formed. The Allende WL rim patterns are instead more likely to result from the effects of secondary processing on the parent body. Alternatively, it could be suggested that the O isotopic variations observed by Simon et al. (2011) were introduced by rapid heating processes in the solar accretion disk as described above. In any case, as the effects of secondary alteration or exchange on the O isotope compositions cannot be ruled out for this CAI, there is no reason to invoke heterogeneity in the hot innermost regions of the early Solar System and rapid transport of CAIs through the disk to other regions.

This consistency of O isotope composition between core and WL rim minerals has implications for the formation of CV3 CAIs. Melilite retains an O isotopic composition identical to that of the other phases in the core and WL rims of CAIs in unaltered samples of other parent bodies investigated in this study (CO and CR meteorites). This appears to indicate that either type A CAIs that were accreted to the CV3 parent body had a distinct origin to those found on other chondritic parent bodies, or that the melilite O isotope variation was a result of processes on the CV3 parent body. It has often been suggested that all CAIs formed in a common source region before being dispatched to their parent bodies (e.g. Krot et al., 2009 and references therein). Such a common origin is further supported by the uniform isotopic composition of the core minerals (with the exception of CV3 melilite) and the WL rims in all the CAIs studied here and, therefore, a distinct origin for CV3 CAIs appears unlikely and provides strong constraints on any models requiring modification of the gaseous reservoir during CAI formation and before WL rim formation. No evidence of isotopic mixing of reservoirs or variable WL rim O isotopic composition is apparent, except for the melilite in CV3 CAIs and, therefore, such gas evolution scenarios appear unlikely. As CV meteorite CAIs appear to be the only ones to show such characteristics, it seems reasonable to suggest that CV CAIs and their WL rims formed in the same ^{16}O-rich reservoir as other CAIs and their WL rims, but were modified after WL rim formation. Whether this alteration occurred on the parent body or during transit of the CAIs from the original reservoir to the parent body is unconstrained. However, given the evidence for extensive mixing in the protosolar accretion disk provided by the huge variety of components present in primitive chondrites, and the previous discussion, a parent body setting is preferred for the modification of the melilite.

4.3. Distribution of the ^{16}O-rich reservoir in time and space

Our study shows that CAIs in unaltered meteorites do not show variations in O isotope composition from the core through to the

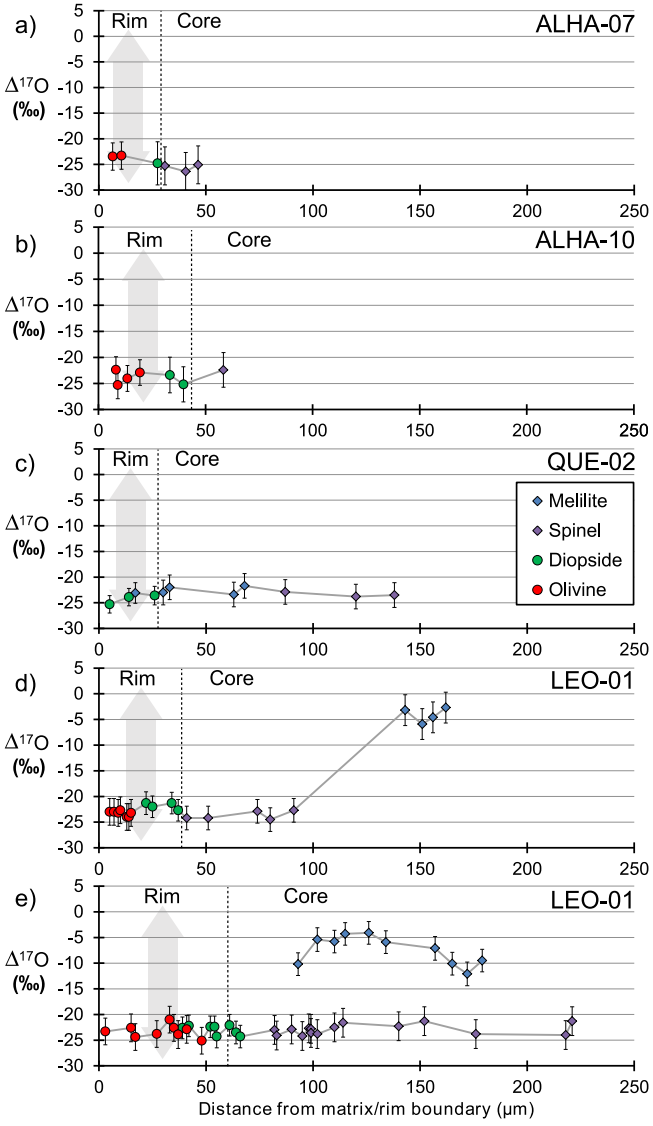

Fig. 7. Oxygen isotope compositions measured across CAI cores and rims (a) ALHA-07 profile a and (b) ALHA-07 profile b, (c) QUE-02 profile c, (d) LEO-01 profile d and (e) LEO-01 profile e. The grey arrows represent the extent of oxygen isotope compositional range in the rim of an Allende CAI reported by Simon et al. (2011) and are given for reference. Legend as in Figs. 4–6. Error bars are shown as 2σ. The distance from the matrix/rim boundary refers to the distance of any given point on the transect nominal line. As availability of suitable analysis locations (e.g. in order to avoid cracks) did not allow for straight profiles, the transects portrayed here represent a section of each CAI. Rim minerals are symbolized by circles and core minerals by diamonds.

WL rims, demonstrating that the O isotopic composition of the inner early Solar System was stable and homogeneous through the formation of Type A CAIs and the development of WL rims. These CAIs were formed over short timescales (Larsen et al., 2011; MacPherson et al., 2012), in a high ambient temperature environment probably near the Sun (e.g. Krot et al., 2009). It is clear that WL rims formed at some point after core formation, at a time when the conditions within that part of the solar accretion disk could have changed.

In addition to the observation of comparable O isotopic compositions in CAIs and their WL rims from three different groups of carbonaceous chondrites, the uniformity of reservoir composition discussed above leads to the conclusion that the ^{16}O-rich reservoir in the early Solar System must have been homogeneous and sufficiently extensive to encompass almost the entire CAI and WL rim formation region and lasted the duration of these formation events. Spinel, the mineral phase most resistant to subsequent isotopic exchange, in almost all CAIs from various chondrite groups displays a restricted range of O isotopic composition, around $\Delta^{17}O = -22‰$ (e.g. Fagan et al., 2004; Aléon et al., 2007; Yoshitake et al., 2005; Itoh et al., 2004). The exception to this is spinel in CH or CB chondrite CAIs that is uniformly ^{16}O-depleted and may result from a late impact induced re-melting event (Krot et al., 2012). Assuming an extensive homogeneous ^{16}O-rich reservoir, there is no reason to invoke any evolution of this reservoir during CAI and WL rim formation, and no evidence that the 5 CAIs studied in the present work moved between reservoirs of different composition. Extremely rare examples of small isotopic heterogeneities are apparent in the inner solar accretion disk, such as two very ^{16}O-rich CAIs from the CH/CB-like meteorite Isheyevo (Gounelle et al., 2009), and a very ^{16}O-rich chondrule in Acfer 214 (Kobayashi et al., 2003). The origin of the more extreme ^{16}O-rich reservoirs remains unclear, but the rarity of such signatures in CAIs and chondrules makes it clear that these cannot have been extensive or common regions, possibly reflecting anomalous gas to dust ratios (Kobayashi et al., 2003), in what was an otherwise homogeneous inner disk with respect to O isotopes.

4.4. Implications for formation of a ^{16}O-rich reservoir and chondrules

The mechanism responsible for the mass independent fractionation of O isotopes required to account for the range in O isotope compositions displayed by Solar System materials remains unclear. Nonetheless, these results seem to favour a mechanism requiring homogeneity in a possibly wide, if localised, area in the inner Solar System, which would require intense mixing and homogenisation in the case of a model involving equilibration between primordial ^{16}O-poor dust and ^{16}O-rich gas (e.g. Krot et al., 2009). Self-shielding of CO has been widely considered as a likely mechanism although there are several locations and specific mechanisms commonly invoked (Clayton, 2002; Yurimoto and Kuramoto, 2004; Lyons and Young, 2005). Chondrules show extensive evidence for formation in a ^{16}O-poor environment (e.g. Clayton et al., 1983; Yurimoto et al., 2008; Connolly and Huss, 2010; Kita et al., 2010; Ushikubo et al., 2012; Schrader et al., 2013; Tenner et al., 2013), and for protracted formation processes starting approximately contemporaneously with CAI formation (Connelly et al., 2012; Itoh and Yurimoto, 2003). It is, therefore, likely that this mass independent fractionation, to more ^{16}O-poor compositions, occurred at a very early stage, possibly overlapping with CAI formation. If there is essentially no evidence for isotopic variation in the inner-most regions of the early disk, this would argue against any mass-independent isotope fractionation mechanisms operating in the vicinity of, and at the same time as, CAI and WL rim formation. This would exclude models invoking fractionation effects at the X-wind location (e.g. Clayton, 2002), and so formation of the ^{16}O-poor reservoir must have occurred further out in the protoplanetary disk. If chondrules were forming at the same time as CAIs, and these early chondrules display O isotopic signatures typical of most chondrules, then chondrule formation must have occurred at a location sufficiently distant from the CAI-forming region as to prevent mixing of O isotope reservoirs, at least during the CAI and WL rim formation phase. These results support the notion that most CAIs formed in a common, localised region and that CAIs remained in this region until at least the end of WL rim formation.

5. Conclusions

High-precision O isotopic spot analyses in the core and WL rims of 5 CAIs from unaltered meteorites belonging to three different groups of carbonaceous chondrites (CO, CV, CR) show that

these CAIs and their WL rims formed in a single O isotopic reservoir. Thus, no transport of these CAIs from one O isotope reservoir to another between the times of core and WL rim formation is required to explain their O isotopic compositions. These results also imply that variations observed previously in the O isotopic compositions across WL rims of a type A CAI from the Allende meteorite are most likely due to secondary processes occurring on the Allende parent body by aqueous alteration and that melilite in CV3 CAIs acquired its ^{16}O-poor composition after WL rim formation.

Homogeneity in the O isotope results for CAIs from three different groups of carbonaceous chondrites supports the hypothesis that CAIs and their rims formed in the same source region and implies that the ^{16}O-rich component was homogeneously distributed in the inner Solar System where CAIs formed and that this region was probably localised, close to the proto-Sun. This reservoir must have persisted until at least the end of WL rim formation.

Additional information

The authors declare that they have no competing financial interests.

Author contributions

All authors discussed the results and implications and contributed to the preparation of the manuscript. I.A.F. and N.A.S. conceived the study and led NanoSIMS measurements. J.-D.B. performed sample characterisation and NanoSIMS measurements. S.S.R. led sample characterisation.

Acknowledgements

We would like to thank the STFC for the studentship for J.-D.B. (grant #ST/J500811/1) and funding for I.A.F., I.P.W. and N.A.S. (grant #ST/1001964/1). NanoSIMS access was via UKCAN. NASA and NHM (London) are thanked for providing samples. Pete Landsberg is thanked for his help with sample and standard preparation as is Diane Johnson for her help with the FIB-SEM. Sam Hammond's and Susanne Schwenzer's help with the electron microprobe is also greatly appreciated. Dr. Alexander Krot, Takayuki Ushikubo and an anonymous reviewer are also thanked for their suggestions that helped greatly in improving this article.

Appendix A. Supplementary material

Supplementary material related to this article can be found online at http://dx.doi.org/10.1016/j.epsl.2014.05.035.

References

Abreu, N.M., 2013. A unique omphacite, amphibole, and graphite-bearing clast in Queen Alexandra Range (QUE) 99177: a metamorphosed xenolith in a pristine CR3 chondrite. Geochim. Cosmochim. Acta 105, 56–72.

Abreu, N.M., Brearley, A.J., 2010. Early solar system processes recorded in the matrices of two highly pristine CR3 carbonaceous chondrites, MET 00426 and QUE 99177. Geochim. Cosmochim. Acta 74, 1146–1171.

Aléon, J., Krot, A.N., McKeegan, K.D., 2002. Calcium–aluminum-rich inclusions and amoeboid olivine aggregates from the CR carbonaceous chondrites. Meteorit. Planet. Sci. 37, 1729–1755.

Aléon, J., El Goresy, A., Zinner, E., 2007. Oxygen isotope heterogeneities in the earliest protosolar gas recorded in a meteoritic calcium–aluminum-rich inclusion. Earth Planet. Sci. Lett. 263, 114–127.

Amelin, Y., Krot, A.N., Hutcheon, I.D., Ulyanov, A.A., 2002. Lead isotopic ages of chondrules and calcium–aluminum-rich inclusions. Science 297, 1678–1683.

Bonal, L., Alexander, C.M.O'D., Huss, G.R., Nagashima, K., Quirico, E., Beck, P., 2013. Hydrogen isotopic composition of the water in CR chondrites. Geochim. Cosmochim. Acta 106, 111–133.

Brearley, A.J., 1997. Disordered biopyriboles, amphibole, and talc in the allende meteorite: products of nebular or parent body aqueous alteration? Science 276, 1103–1105.

Chizmadia, L.J., Rubin, A.E., Wasson, J.T., 2002. Mineralogy and petrology of amoeboid olivine inclusions in CO3 chondrites: relationship to parent-body aqueous alteration. Meteorit. Planet. Sci. 37, 1781–1796.

Choi, B.-G., Krot, A.N., Wasson, J.T., 2000. Oxygen isotopes in magnetite and fayalite in CV chondrites Kaba and Mokoia. Meteorit. Planet. Sci. 35, 1239–1248.

Clayton, R.N., 2002. Self-shielding in the solar nebula. Nature 415, 860–861.

Clayton, R.N., Onuma, N., Grossman, L., Mayeda, T.K., 1977. Distribution of the presolar component in allende and other carbonaceous chondrites. Earth Planet. Sci. Lett. 34, 209–224.

Clayton, R.N., Onuma, N., Ikeda, Y., Mayeda, T.K., Hutcheon, I.D., Olsen, E.J., Molini-Velsko, C., 1983. Oxygen isotopic compositions of chondrules in allende and ordinary chondrites. In: King, E.A. (Ed.), Chondrules and their Origins. The Lunar and Planetary Institute, Houston, pp. 37–43.

Connelly, J.N., Bizzarro, M., Krot, A.N., Nordlund, Å, Wielandt, D., Ivanova, M.A., 2012. The absolute chronology and thermal processing of solids in the solar protoplanetary disk. Science 338, 651–655.

Connolly Jr., H.C., Huss, G.R., 2010. Compositional evolution of the protoplanetary disk: oxygen isotopes of type-II chondrules from CR2 chondrites. Geochim. Cosmochim. Acta 74, 2473–2483.

Cosarinsky, M., Leshin, L.A., MacPherson, G.J., Guan, Y., Krot, A.N., 2008. Chemical and oxygen isotopic compositions of accretionary rim and matrix olivine in CV chondrites: constraints on the evolution of nebular dust. Geochim. Cosmochim. Acta 72, 1887–1913.

Fagan, T.J., Krot, A.N., Keil, K., Yurimoto, H., 2004. Oxygen isotopic alteration in Ca–Al-rich inclusions from Efremovka: nebular or parent body setting? Meteorit. Planet. Sci. 39, 1257–1272.

Fagan, T.J., Guan, Y., MacPherson, G.J., 2007. Al–Mg isotopic evidence for episodic alteration of Ca–Al-rich inclusions from Allende. Meteorit. Planet. Sci. 42, 1221–1240.

Gounelle, M., Krot, A.N., Nagashima, K., Kearsley, A., 2009. Extreme ^{16}O enrichment in calcium–aluminum-rich inclusions from the Isheyevo (CH/CB) chondrite. Astrophys. J. 698, L18–L22.

Greenwood, J.P., 2004. Disequilibrium melting of refractory inclusions: a mechanism for high-temperature oxygen isotope exchange in the solar nebula. Lunar Planet. Sci. 36 (abstract #2132).

Harazono, K., Yurimoto, H., 2003. Oxygen isotopic variations in a fluffy type A CAI from the Vigarano meteorite. Lunar Planet. Sci. 34 (abstract #1540).

Hoppe, P., Cohen, S., Meiborn, A., 2013. NanoSIMS: technical aspects and applications in cosmochemistry and biological geochemistry. Geostand. Geoanal. Res. 37, 111–154.

Hua, X., Huss, G.R., Tachibana, S., Sharp, T.G., 2004. Oxygen, silicon, and Mn–Cr isotopes of fayalite in the Kaba oxidized CV3 chondrite: constraints for its formation history. Geochim. Cosmochim. Acta 69, 1333–1348.

Ito, M., Nagasawa, H., Yurimoto, H., 2004. Oxygen isotopic SIMS analysis in Allende CAI: details of the very early thermal history of the solar system. Geochim. Cosmochim. Acta 68, 2905–2923.

Itoh, S., Yurimoto, H., 2003. Contemporaneous formation of chondrules and refractory inclusions in the early Solar System. Nature 423, 728–731.

Itoh, S., Kojima, H., Yurimoto, H., 2004. Petrography and oxygen isotopic compositions in refractory inclusions from CO chondrites. Geochim. Cosmochim. Acta 68, 183–194.

Jogo, K., Nagashima, K., Hutcheon, I.D., Krot, A.N., Nakamura, T., 2013. Heavily metamorphosed clasts from the CV chondrite breccias Mokoia and Yamato-86009. Meteorit. Planet. Sci. 47, 2251–2268.

Katayama, J., Itoh, S., Yurimoto, H., 2012. Oxygen isotopic zoning of reversely zoned melilite crystals in a fluffy type A Ca–Al-rich inclusions from the Vigarano meteorite. Meteorit. Planet. Sci. 47, 2094–2106.

Kawasaki, N., Sakamoto, N., Yurimoto, H., 2012. Oxygen isotopic and chemical zoning of melilite crystals in a type A Ca–Al-rich inclusion of Efremovka CV3 chondrite. Meteorit. Planet. Sci. 47, 2084–2093.

Kita, N.T., Nagahara, H., Tachibana, S., Tomomura, S., Spicuzza, M.J., Fournelle, J.H., Valley, J.W., 2010. High precision SIMS oxygen three isotope study of chondrules in LL3 chondrites: role of ambient gas during chondrule formation. Geochim. Cosmochim. Acta 74, 6610–6635.

Kobayashi, S., Imai, H., Yurimoto, H., 2003. New extreme ^{16}O-rich reservoir in the early solar system. Geochem. J. 37, 663–669.

Krot, A.N., MacPherson, G.J., Ulyanov, A.A., Petaev, M.I., 2004. Fine-grained, spinel-rich inclusions from the reduced CV chondrites Efremovka and Leoville: I. Mineralogy, petrology, and bulk chemistry. Meteorit. Planet. Sci. 39, 1517–1553.

Krot, A.N., Amelin, Y., Bland, P., Ciesla, F.J., Connelly, J., Davis, A.M., Huss, G.R., Hutcheon, I.D., Makide, K., Nagashima, K., Nyquist, L.E., Russell, S.S., Scott, E.R.D., Thrane, K., Yurimoto, H., Yin, Q.-Z., 2009. Origin and chronology of chondritic components: a review. Geochim. Cosmochim. Acta 73, 4963–4997.

Krot, A.N., Nagashima, K., Petaev, M.I., 2012. Isotopically uniform, ^{16}O-depleted calcium, aluminium-rich inclusions in CH and CB carbonaceous chondrites. Geochim. Cosmochim. Acta 83, 159–178.

Larsen, K.K., Trinquier, A., Paton, C., Schiller, M., Wielandt, D., Ivanova, M.A., Connelly, J.N., Nordlund, Å., Krot, A.N., Bizzarro, M., 2011. Evidence for magnesium isotope heterogeneity in the solar protoplanetary disk. Astrophys. J. 735, L37–L43.

Lyons, J.R., Young, E.D., 2005. CO self-shielding as the origin of oxygen isotope anomalies in the early solar nebula. Nature 435, 317–320.

MacPherson, G.J., Grossman, L., 1984. "Fluffy" type A Ca-, Al-rich inclusions in the Allende meteorite. Geochim. Cosmochim. Acta 48, 29–46.

MacPherson, G.J., Krot, A.N., 2002. Distribution of Ca–Fe-silicates in CV3 chondrites: possible controls by parent-body compaction. In: 65th Annual Meteoritical Society Meeting.

MacPherson, G.J., Simon, S.B., Davis, A.M., Grossman, L., Krot, A.N., 2005. Calcium–aluminum-rich inclusions: major unanswered questions. In: Krot, A.N., Scott, E.R.D., Reipurth, B. (Eds.), Chondrites and the Protoplanetary Disk. Astronomical Society of the Pacific, Hawai'i, pp. 225–250.

MacPherson, G.J., Kita, N.T., Ushikubo, T., Bullock, E.S., Davis, A.M., 2012. Well-resolved variations in the formation ages for Ca–Al-rich inclusions in the early Solar System. Earth Planet. Sci. Lett. 331–332, 43–54.

Maruyama, S., Yurimoto, H., Shigeho, S., 1999. Oxygen isotope evidence regarding the formation of spinel-bearing chondrules. Earth Planet. Sci. Lett. 169, 165–171.

McKeegan, K.D., Kallio, A.P.A., Heber, V.S., Jarzebinski, G., Mao, P.H., Coath, C.D., Kunihiro, T., Wiens, R.C., Nordholt, J.E., Moses, R.W., Reisenfeld, D.B., Jurewicz, A.J.G., Burnett, D.S., 2011. The oxygen isotopic composition of the Sun inferred from captured solar wind. Science 332, 1528–1532.

Miller, M.F., Franchi, I.A., Sexton, A.S., Pillinger, C.T., 1999. High precision $\delta^{17}O$ isotope measurements of oxygen from silicates and other oxides: method and applications. Rapid Commun. Mass Spectrom. 13, 1211–1217.

Rowe, M.W., Clayton, R.N., Mayeda, T.K., 1994. Oxygen isotopes in separated components of CI and CM meteorites. Geochim. Cosmochim. Acta 58, 5341–5347.

Rudraswami, N.G., Ushikubo, T., Nakashima, D., Kita, N.T., 2011. Oxygen isotope systematics of chondrules in the Allende CV3 chondrite: high precision ion microprobe studies. Geochim. Cosmochim. Acta 75, 7596–7611.

Schrader, D.L., Franchi, I.A., Connolly Jr., H.C., Greenwood, R.C., Lauretta, D.S., Gibson, J.N., 2011. The formation and alteration of the Renazzo-like carbonaceous chondrites I: implications of bulk-oxygen isotopic composition. Geochim. Cosmochim. Acta 75, 308–325.

Schrader, D.L., Connolly Jr., H.C., Lauretta, D.S., Nagashima, K., Huss, G.R., Davidson, J., Domanik, K.J., 2013. The formation and alteration of the Renazzo-like carbonaceous chondrites II: linking O-isotope composition and oxidation state of chondrule olivine. Geochim. Cosmochim. Acta 101, 302–327.

Scott, E.R.D., Jones, R.H., 1990. Disentangling nebular and asteroidal features of CO3 carbonaceous chondrite meteorites. Geochim. Cosmochim. Acta 54, 2485–2502.

Simon, J.I., Young, E.D., Russell, S.S., Tonui, E.K., Dyl, K.A., Manning, C.E., 2005. A short timescale for changing oxygen fugacity in the solar nebula revealed by high-resolution ^{26}Al–^{26}Mg dating of CAI rims. Earth Planet. Sci. Lett. 238, 272–283.

Simon, S.B., Sutton, S.R., Grossman, L., 2007. Valence of titanium and vanadium in pyroxene in refractory inclusion interiors and rims. Geochim. Cosmochim. Acta 71, 3098–3118.

Simon, J.I., Hutcheon, I.D., Simon, S.B., Matzel, J.E.P., Ramon, E.C., Weber, P.K., Grossman, L., DePaolo, D.J., 2011. Oxygen isotope variations at the margin of a CAI records circulation within the Solar Nebula. Science 331, 1175–1178.

Starkey, N.A., Franchi, I.A., 2013. Insight into the silicate and organic reservoirs of the comet forming region. Geochim. Cosmochim. Acta 105, 73–91.

Stolper, E., 1982. Crystallization sequences of Ca–Al-rich inclusions from Allende: an experimental study. Geochim. Cosmochim. Acta 46, 2159–2180.

Tenner, T.J., Ushikubo, T., Kurahashi, E., Kita, N.T., Nagahara, H., 2013. Oxygen isotope systematic of chondrule phenocrysts from the CO3.0 chondrite Yamato 81020: evidence for two distinct oxygen isotope reservoirs. Geochim. Cosmochim. Acta 102, 226–245.

Ushikubo, T., Kimura, M., Kita, N.T., Valley, J.W., 2012. Primordial oxygen isotope reservoirs of the solar nebula recorded in chondrules in Acfer 094 carbonaceous chondrites. Geochim. Cosmochim. Acta 90, 242–264.

Wark, D.A., Boynton, W.V., 2001. The formation of rims on calcium–aluminum-rich inclusions: step I – flash heating. Meteorit. Planet. Sci. 36, 1135–1166.

Wark, D.A., Lovering, J.F., 1977. Marker events in the early evolution of the solar system: evidence from rims on Ca–Al-rich inclusions in carbonaceous chondrites. Proc. Lunar Sci. Conf. 8, 95–112.

Yoshitake, M., Koide, Y., Yurimoto, H., 2005. Correlations between oxygen-isotopic composition and petrologic setting in a coarse-grained Ca, Al-rich inclusion. Geochim. Cosmochim. Acta 69, 2663–2674.

Young, E.D., Russell, S.S., 1998. Oxygen reservoirs in the early Solar Nebula inferred from an Allende CAI. Science 282, 452–455.

Young, E.D., Simon, J.I., Galy, A., Russell, S.S., Tonui, E., Lovera, O., 2005. Supracanonical $^{26}Al/^{27}Al$ and the residence time of CAIs in the solar protoplanetary disk. Science 308, 223–227.

Yurimoto, H., Kuramoto, K., 2004. Molecular cloud origin for the oxygen isotope heterogeneity in the Solar System. Science 305, 1763–1766.

Yurimoto, H., Ito, M., Nagasawa, H., 1998. Oxygen isotope exchange between refractory inclusion in Allende and Solar Nebula gas. Science 282, 1874–1877.

Yurimoto, H., Krot, A.N., Choi, B.-G., Aléon, J., Kunihiro, T., Brearley, A.J., 2008. Oxygen isotopes of chondritic components. In: Rosso, J.J. (Ed.), Oxygen in the Solar System. In: Reviews Mineralogy & Geochemistry, vol. 68. Mineralogical Society of America, Washington DC, pp. 141–186.